Electronic Supplementary Information:

CO_2 conversion in a dielectric barrier discharge plasma: N_2 in the mix as helping hand or problematic impurity?

Ramses Snoeckx,[1] Stijn Heijkers,[1] Karen Van Wesenbeeck,[2] Silvia Lenaerts[2] and Annemie Bogaerts[1]

[1]Research group PLASMANT, Department of Chemistry, University of Antwerp, Universiteitsplein 1, BE-2610 Antwerp, Belgium

[2]Research group DuEL, Department of Bioscience Engineering, University of Antwerp, Antwerp, Belgium

E-mail: ramses.snoeckx@uantwerpen.be

1. Detailed experimental results

1.1. CO_2 and N_2 conversion

The experimental results presented here are first shown without correction for the gas expansion factor (i.e. raw data). The corrected experimental results are presented in section 1.1.2.

The experimental procedure consists of stabilizing the plasma for 30 minutes, followed by 5 consecutive measurements with the compact gas chromatograph (CGC), which take 2 minutes per measurement, and at the same time recording the peak-to-peak voltage and power, and finally a cool down and flush period of 20 minutes with the next gas mixture. The results shown below are thus the average of these 5 consecutive measurements. All measurements were performed at an applied frequency of 23.5 kHz.

The measurements were performed in three series: a) adding 0-10 % N_2 in steps of 1 %; b) adding 0-90 % N_2 in steps of 10 %; c) adding 90-98 % N_2, again in steps of 1 %.

1.1.1. Raw data

The following tables give the CO_2 and N_2 flow rates in ml/min (1st and 2nd colum), the corresponding CO_2 and N_2 percentages in the mixture (3rd and 4th column), the average peak-to-peak voltage (column 5), the average plasma power (column 6), the average CO_2 conversion with standard deviation (column 7 and 8), the average N_2 conversion with

standard deviation (column 9 and 10), the average energy cost per converted CO_2 molecule (column 11) and the obtained average energy efficiency (column 12).

a) 0-10 % N_2

CO_2 (ml/min)	N_2 (ml/min)	CO_2 (%)	N_2 (%)	Vp-p (kV)	Power (W)	χ CO_2 (%)	σ CO_2 (%)	χ N_2 (%)	σ N_2 (%)	Energy Cost (eV/molec)	η (%)
611	0	100	0	11.67	121.9	4.88	0.30	-	-	37.4	5.1
605	6.1	99	1	11.73	123.1	6.21	0.27	3.06	1.44	29.7	6.4
599	12.2	98	2	11.75	121.4	6.04	0.36	8.15	3.98	30.9	6.2
593	18.3	97	3	11.74	122.8	6.14	0.30	5.04	1.01	30.7	6.2
587	24.4	96	4	11.79	122.7	6.15	0.32	2.55	1.20	30.9	6.1
580	30.5	95	5	11.80	124.7	6.42	0.28	3.19	1.85	30.0	6.3
574	36.6	94	6	11.86	125.6	6.47	0.30	2.10	1.36	30.1	6.1
567	42.8	93	7	11.87	126.8	6.70	0.31	2.12	1.31	29.3	6.2
562	48.9	92	8	11.88	125.8	6.75	0.33	2.77	1.22	29.5	6.3
556	55.0	91	9	11.91	125.7	6.79	0.30	1.91	1.28	29.6	6.2
550	61.1	90	10	11.93	126.9	6.81	0.28	2.99	1.80	29.8	6.1

b) 0-90 % N_2

CO_2 (ml/min)	N_2 (ml/min)	CO_2 (%)	N_2 (%)	Vp-p (kV)	Power (W)	χ CO_2 (%)	σ CO_2 (%)	χ N_2 (%)	σ N_2 (%)	Energy Cost (eV/molec)	η (%)
611	0	100	0	11.73	122.8	4.74	0.03	-	-	59.1	4.9
550	61	90	10	11.83	123.5	6.77	0.20	2.96	0.22	46.3	6.3
489	122	80	20	11.89	124.2	6.98	0.25	2.08	0.67	50.7	5.7
428	183	70	30	11.93	123.5	7.66	0.28	2.67	0.59	52.6	5.5
367	244	60	40	12.00	121.5	8.51	0.26	2.38	0.54	54.3	5.4
305	305	50	50	12.05	122.0	9.42	0.27	2.36	0.43	59.2	4.9
244	366	40	60	12.05	120.7	10.72	0.31	2.35	0.36	64.4	4.5
183	428	30	70	12.14	122.1	12.43	0.23	1.97	0.31	74.9	3.9
122	489	20	80	12.22	118.3	14.95	0.24	1.84	0.32	90.4	3.2
61	550	10	90	12.07	116.9	19.07	0.20	1.21	0.34	140.1	2.1

c) 90-98 % N_2

CO_2 (ml/min)	N_2 (ml/min)	CO_2 (%)	N_2 (%)	Vp-p (kV)	Power (W)	χ CO_2 (%)	σ CO_2 (%)	χ N_2 (%)	σ N_2 (%)	Energy Cost (eV/molec)	η (%)
61	550	10	90	11.75	116.7	19.19	0.21	1.16	0.34	138.9	2.1
55	546	9	91	11.67	114.2	19.55	0.32	1.29	0.31	148.2	2.0
49	562	8	92	11.65	115.4	20.18	0.27	1.16	0.35	162.7	1.8
43	568	7	93	11.55	116.2	20.91	0.32	0.99	0.31	180.1	1.6
37	574	6	94	11.51	114.6	21.58	0.30	0.95	0.31	200.1	1.5
31	580	5	95	11.42	110.6	22.22	0.34	0.71	0.31	224.0	1.3
24	586	4	96	11.40	111.1	23.52	0.26	0.73	0.30	274.3	1.1
18	592	3	97	11.25	110.8	24.34	0.40	0.18	0.31	352.5	0.8
12	599	2	98	11.51	109.9	25.72	0.39	0.45	0.35	496.5	0.6

1.1.2. Correction for gas expansion

In this section the obtained experimental results corrected for the gas expansion are presented; these corrected results are the data used throughout the manuscript.

In this work the corrected results are obtained by performing an iterative back calculation, with the following assumptions: (i) CO_2 is split into CO and ½ O_2, so every converted CO_2 molecule gives rise to an expansion of the volume by a factor 1.5. (ii) On the other hand, for N_2, due to its low conversion, we assume that the conversion of N_2 does not contribute to the gas expansion.

Based on these two assumptions we start from the "faulty" conversions obtained from our GC measurements. We know that the gas expanded and since we have a sample loop with a fixed volume, this means that the pressure increases. However, since our GC samples at atmospheric pressure, part of the gas is lost due to the depressurization in the GC system before injection, leaving less molecules in the sample volume than originally present in the outlet flow. Since there are now less (CO_2 and N_2) molecules in the sample, the (CO_2 and N_2) conversion will appear higher. To correct for this, we calculate X_{GC} by solving the equation below for different values of X_{Real} until X_{GC} matches the (CO_2 or N_2) conversion measured by the GC.

$$X_{GC} = 1 - \left(\frac{1 - X_{Real}}{1 + \alpha\left(\frac{X_{Real}}{2}\right)} \right) \quad (1)$$

This formula is used for both the CO_2 and N_2 conversion. The derivation of it, in case of CO_2, is explained below. In this formula X_{GC} is the calculated conversion, which we expect to be measured by the GC due to the gas expansion for a certain value of X_{Real}, which is the real conversion.

This equation is derived, on one hand, from the expression to calculate the remaining fraction of (CO_2 or N_2) in the output:

$$Fraction\ (output) = (1 - X_{Real}) \quad (2)$$

And on the other hand, from the expression for the gas expansion due to the CO_2 conversion:

$$Gas\ expansion = 1 + \alpha \left(\frac{X_{Real}}{2}\right) \quad (3)$$

In the latter expression, according to our first assumption, $\alpha(X_{Real}/2)$ accounts for the gas expansion due to the CO_2 conversion, as this corresponds to the O_2 formed for a certain CO_2 conversion (X_{Real}), where α is the fraction of CO_2 in the initial (CO_2/N_2) gas mixture. Furthermore, according to the second assumption, the N_2 conversion does not give rise to further volume expansion.

Dividing expression 2 by expression 3 tells us how the output is normalized due to the depressurization in the CGC system, and subtracting this value from one, ultimately gives us the "faulty" conversion as obtained in the CGC under influence of the gas expansion. Thus by

doing this calculation for a range of different X_{Real} values and matching X_{GC} to the measured "faulty" conversion by the GC, we can determine the "real" CO_2 conversion, X_{Real}.

After calculating X_{Real} for CO_2, we can calculate the "real" conversion for N_2 following the same procedure. In this case, X_{Real} in expression 2 stands for the N_2 conversion, while X_{Real} in expression 3 is the already calculated "real" conversion of CO_2.

The following tables give the CO_2 and N_2 flow rates in ml/min (1st and 2nd column), the corresponding CO_2 and N_2 percentages in the mixture (3rd and 4th column), the average experimental CO_2 conversion before and after correction for the gas expansion (5th and 6th column), the average experimental N_2 conversion before and after correction for the gas expansion (7th and 8th column), the average experimental energy efficiency before and after correction for the gas expansion(9th and 10th column).

a) 0-10 % N_2

CO_2 (ml/min)	N_2 (ml/min)	CO_2 (%)	N_2 (%)	χ CO_2 (%)	χ CO_2 Gas exp (%)	χ N_2 (%)	χ N_2 Gas exp (%)	η (%)	η Gas exp (%)
611	0	100	0	4.88	3.30	-	-	5.1	3.5
605	6.1	99	1	6.21	4.24	3.06	1.02	6.4	4.3
599	12.2	98	2	6.04	4.14	8.15	-	6.2	4.3
593	18.3	97	3	6.14	4.22	5.04	-	6.2	4.2
587	24.4	96	4	6.15	4.24	2.55	0.57	6.1	4.2
580	30.5	95	5	6.42	4.44	3.19	1.15	6.3	4.3
574	36.6	94	6	6.47	4.49	2.10	0.03	6.1	4.3
567	42.8	93	7	6.70	4.68	2.12	-	6.2	4.4
562	48.9	92	8	6.75	4.72	2.77	0.66	6.3	4.4
556	55.0	91	9	6.79	4.77	1.91	-	6.2	4.4
550	61.1	90	10	6.81	4.80	2.99	0.90	6.1	4.3

b) 0-90 % N_2

CO_2 (ml/min)	N_2 (ml/min)	CO_2 (%)	N_2 (%)	χ CO_2 (%)	χ CO_2 Gas exp (%)	χ N_2 (%)	χ N_2 Gas exp (%)	η (%)	η Gas exp (%)
611	0	100	0	4.74	3.21	-	-	4.9	3.3
550	61	90	10	6.77	4.77	2.96	0.10	6.3	4.4
489	122	80	20	6.98	5.09	2.08	0.09	5.7	4.2
428	183	70	30	7.66	5.79	2.67	0.70	5.5	4.2
367	244	60	40	8.51	6.67	2.38	0.42	5.4	4.2
305	305	50	50	9.42	7.68	2.36	0.49	4.9	4.0
244	366	40	60	10.72	9.10	2.35	0.58	4.5	3.8
183	428	30	70	12.43	10.99	1.97	0.36	3.9	3.4
122	489	20	80	14.95	13.78	1.84	0.49	3.2	3.0
61	550	10	90	19.07	18.33	1.21	0.31	2.1	2.0

c) 90-98 % N_2

CO_2 (ml/min)	N_2 (ml/min)	CO_2 (%)	N_2 (%)	χ CO_2 (%)	χ CO_2 Gas exp (%)	χ N_2 (%)	χ N_2 Gas exp (%)	η (%)	η Gas exp (%)
61	550	10	90	19.19	18.45	1.16	0.25	2.1	2.0
55	546	9	91	19.55	18.86	1.29	0.45	2.0	1.9
49	562	8	92	20.18	19.55	1.16	0.38	1.8	1.7
43	568	7	93	20.91	20.34	0.99	0.28	1.6	1.6
37	574	6	94	21.58	21.08	0.95	0.32	1.5	1.4
31	580	5	95	22.22	21.79	0.71	0.16	1.3	1.3
24	586	4	96	23.52	23.18	0.73	0.28	1.1	1.0
18	592	3	97	24.34	24.07	0.18	-	0.8	0.8
12	599	2	98	25.72	25.53	0.45	0.20	0.6	0.6

1.2. NO_x formation

To study the formation of O_3, N_2O and NO_x compounds, we applied Fourier transform infrared spectroscopy (FTIR). FTIR bands corresponding to an IR active functional group of the gases are monitored in real-time. Figure 1 shows the spectrum for a 50-50 mixture CO_2/N_2 with the different bands indicated.

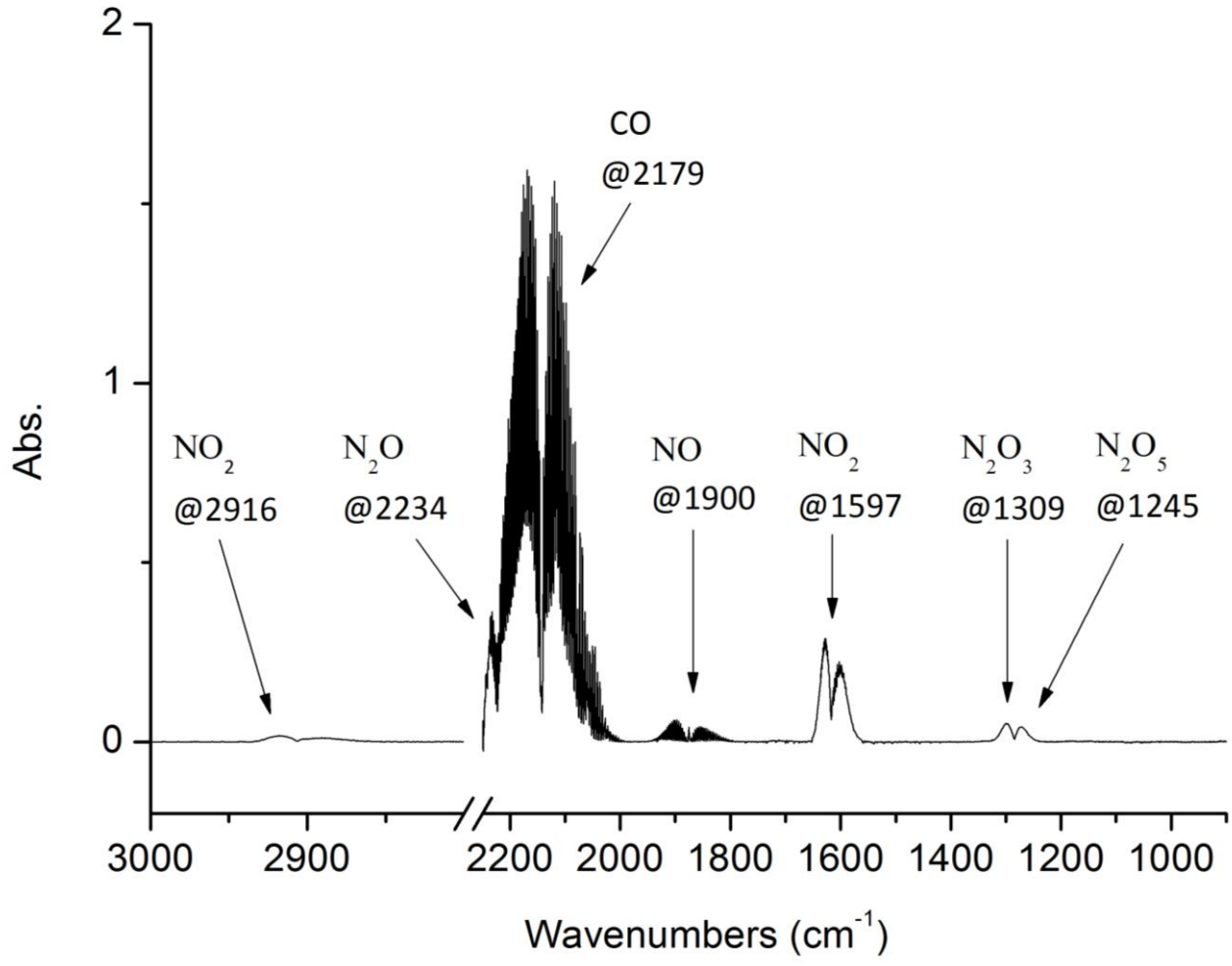

Figure 1. FTIR spectrum for a 50-50 mixture CO_2/N_2, indicating the different NO_x (and N_2O and CO) logging bands.

1.2.1. Raw data

The following tables give the CO_2 and N_2 flow rates in ml/min (1st and 2nd column), the corresponding CO_2 and N_2 percentages in the mixture (3rd and 4th column), the NO band (νNO) at 1900 cm^{-1} (column 5), the NO_2 ($\nu_{as}NO_2$) band logging at 1597 cm^{-1} (column 6), the NO_2 ($\nu_{as}NO_2 + \nu_sNO_2$) band logging at 2916 cm^{-1} (column 7), the N_2O band logging (νNN at 2234 cm^{-1}) (column 8), the N_2O_3 band logging (ν_sNO_2 at 1309 cm^{-1}) (column 9) and the N_2O_5 band logging (ν_sNO_2 at 1245 cm^{-1}) (column 10). Note that all these results are in arbitrary units (a.u.). Ozone (ν_s at 1054 cm^{-1}) was never detected with the FTIR spectrometer.

a) 0-10 % N_2

CO_2 (ml/min)	N_2 (ml/min)	CO_2 (%)	N_2 (%)	NO 1900 cm^{-1} (a.u.)	NO_2 1597 cm^{-1} (a.u.)	NO_2 2916 cm^{-1} (a.u)	N_2O 2234 cm^{-1} (a.u.)	N_2O_3 1309 cm^{-1} (a.u.)	N_2O_5 1245 cm^{-1} (a.u.)
611	0	100	0	-0.00253	-1.7E-05	7.34E-05	0.036386	-0.00041	-8.3E-05
605	6.1	99	1	0.012213	0.031595	0.002923	0.039362	0.000924	-0.00015
599	12.2	98	2	0.021533	0.039766	0.003497	0.043622	0.000685	-8.4E-05
593	18.3	97	3	0.029751	0.045549	0.003799	0.042921	0.000624	-0.00012
587	24.4	96	4	0.034032	0.049059	0.004175	0.039506	0.000466	-0.00012
580	30.5	95	5	0.041603	0.056878	0.004826	0.051976	0.000654	2.8E-05
574	36.6	94	6	0.047258	0.061017	0.005179	0.041416	0.00058	1.86E-05
567	42.8	93	7	0.055974	0.019795	0.001697	0.030233	-0.00044	-0.01203
562	48.9	92	8	0.060648	0.071408	0.005958	0.058815	0.000231	-0.00014
556	55.0	91	9	0.066247	0.075564	0.006115	0.051033	0.000674	-6.2E-05
550	61.1	90	10	0.066589	0.079807	0.006598	0.061262	0.000458	0.000105

b) 0-100 % N_2

CO_2 (ml/min)	N_2 (ml/min)	CO_2 (%)	N_2 (%)	NO 1900 cm^{-1} (a.u.)	NO_2 1597 cm^{-1} (a.u.)	NO_2 2916 cm^{-1} (a.u)	N_2O 2234 cm^{-1} (a.u.)	N_2O_3 1309 cm^{-1} (a.u.)	N_2O_5 1245 cm^{-1} (a.u.)
611	0	100	0	-0.00253	-1.7E-05	7.34E-05	0.036386	-0.00041	-8.3E-05
550	61	90	10	0.066589	0.079807	0.006598	0.061262	0.000458	0.000105
489	122	80	20	0.11901	0.124921	0.010034	0.069467	0.002137	0.000209
428	183	70	30	0.130232	0.136295	0.011263	0.075507	0.003043	0.000378
367	244	60	40	0.166776	0.160221	0.013264	0.108849	0.006826	0.000638
305	305	50	50	0.169517	0.169624	0.014203	0.097302	0.005478	0.00081
244	366	40	60	0.154286	0.149847	0.012222	0.093913	0.005511	0.000601
183	428	30	70	0.13485	0.124089	0.009329	0.0964	0.006807	0.00071
122	489	20	80	0.121135	0.095289	0.007561	0.092582	0.007864	0.000922
61	550	10	90	0.060983	0.041701	0.003382	0.06438	0.006069	0.000389
0	611	0	100	0.000111	0.000234	-0.00034	0.031113	0.003044	-6.7E-05

c) 90-98 % N_2

CO_2 (ml/min)	N_2 (ml/min)	CO_2 (%)	N_2 (%)	NO 1900 cm^{-1} (a.u.)	NO_2 1597 cm^{-1} (a.u.)	NO_2 2916 cm^{-1} (a.u)	N_2O 2234 cm^{-1} (a.u.)	N_2O_3 1309 cm^{-1} (a.u.)	N_2O_5 1245 cm^{-1} (a.u.)
61	550	10	90	0.060983	0.041701	0.003382	0.06438	0.006069	0.000389
55	546	9	91	0.039257	0.027067	0.00189	0.063275	0.006361	0.0005
49	562	8	92	0.029098	0.020959	0.001361	0.060787	0.00611	0.000613
43	568	7	93	0.025768	0.01792	0.001039	0.053	0.005325	0.000529
37	574	6	94	0.012127	0.013251	0.000913	0.062193	0.005806	0.00065
31	580	5	95	0.000514	0.000591	-0.00035	0.038054	0.003664	8.73E-05
24	586	4	96	0.000451	0.00084	-0.00031	0.039158	0.003677	0.00045
18	592	3	97	0.000275	0.000589	-0.00034	0.035147	0.003209	8.74E-05
12	599	2	98	0.000293	0.000568	-0.00046	0.034365	0.003356	0.000332

1.2.2. NO and NO_2 conversion to ppm

A ChemiLuminescence Detector (CLD) NO/NO_x analyzer module (Emerson Process Managament) was used to prepare a calibration curve for correlating the NO and NO_2 FTIR band intensities to NO and NO_2 concentrations in ppm. The CLD analyzer module determines either NO or combined NO and NO_2. In this way it is possible to link the absorption height to the respective concentrations by using a calibration curve.

The following tables give the CO_2 and N_2 flow rates in ml/min (1st and 2nd colum), the corresponding CO_2 and N_2 percentages in the mixture (3rd and 4th column), the NO band (νNO) at 1900 cm^{-1} in arbitrary units (column 5), and in parts per million (column 6), the NO_2 ($\nu_{as}NO_2$) infrared band logging at 1597 cm^{-1} in arbitrary units (column 7) and in parts per million (column 8).

a) 0-10 % N_2

CO_2 (ml/min)	N_2 (ml/min)	CO_2 (%)	N_2 (%)	NO 1900 cm^{-1} (a.u.)	NO 1900 cm^{-1} (ppm)	NO_2 1597 cm^{-1} (a.u.)	NO_2 1597 cm^{-1} (ppm)
611	0	100	0	-0.00253	-	-1.7E-05	-
605	6.1	99	1	0.012213	39.96	0.031595	9.97
599	12.2	98	2	0.021533	70.46	0.039766	12.54
593	18.3	97	3	0.029751	97.35	0.045549	14.37
587	24.4	96	4	0.034032	111.36	0.049059	15.48
580	30.5	95	5	0.041603	136.14	0.056878	17.94
574	36.6	94	6	0.047258	154.64	0.061017	19.25
567	42.8	93	7	0.055974	183.16	0.019795	-
562	48.9	92	8	0.060648	198.45	0.071408	22.53
556	55.0	91	9	0.066247	216.78	0.075564	23.84
550	61.1	90	10	0.066589	217.90	0.079807	25.18

b) 0-100 % N_2

CO_2 (ml/min)	N_2 (ml/min)	CO_2 (%)	N_2 (%)	NO 1900 cm^{-1} (a.u.)	NO 1900 cm^{-1} (ppm)	NO_2 1597 cm^{-1} (a.u.)	NO_2 1597 cm^{-1} (ppm)
611	0	100	0	-0.00253	-	-1.7E-05	-
550	61	90	10	0.066589	217.90	0.079807	25.18
489	122	80	20	0.11901	389.43	0.124921	39.41
428	183	70	30	0.130232	426.15	0.136295	43.00
367	244	60	40	0.166776	545.73	0.160221	50.54
305	305	50	50	0.169517	554.70	0.169624	53.51
244	366	40	60	0.154286	504.86	0.149847	47.27
183	428	30	70	0.13485	441.26	0.124089	39.14
122	489	20	80	0.121135	396.38	0.095289	30.06
61	550	10	90	0.060983	199.55	0.041701	13.15
0	611	0	100	0.000111	0.36	0.000234	0.07

c) 90-98 % N_2

CO_2 (ml/min)	N_2 (ml/min)	CO_2 (%)	N_2 (%)	NO 1900 cm^{-1} (a.u.)	NO 1900 cm^{-1} (ppm)	NO_2 1597 cm^{-1} (a.u.)	NO_2 1597 cm^{-1} (ppm)
61	550	10	90	0.060983	199.55	0.041701	13.15
55	546	9	91	0.039257	128.46	0.027067	8.54
49	562	8	92	0.029098	95.22	0.020959	6.61
43	568	7	93	0.025768	84.32	0.01792	5.65
37	574	6	94	0.012127	39.68	0.013251	4.18
31	580	5	95	0.000514	1.68	0.000591	0.19
24	586	4	96	0.000451	1.48	0.00084	0.26
18	592	3	97	0.000275	0.90	0.000589	0.19
12	599	2	98	0.000293	0.96	0.000568	0.18

2. Modeling details

2.1 Modeling the filaments/microdischarges in the DBD

We assume that every molecule has passed through a triangular microdischarge pulse of 30 ns every 100 half cycles, adopted from the work of Snoeckx et al.[1] For a residence time of 0.73 s and a frequency of 23.5 kHz, this means that the molecules pass through a microdischarge every 2.1 ms. The average power consumed per microdischarge is equal to the power inserted in the plasma divided by the total number of microdischarges through which the molecules pass. For each microdischarge, the power rises linearly towards a value equal to two times the average power consumed per microdischarge at 15 ns, and decreases again linearly towards zero at 30 ns. The electron density in every microdischarge is held between $10^{12}cm^{-3}$ and $10^{14}cm^{-3}$.[2–4]

2.2. Modeling results

In this section the calculated results from the zero dimensional chemical kinetics model are presented. The same kinetic model as in reference[5] is used with some minor changes (as listed in the following table).

Reaction	**Rate Constant (cm^3*$molecule^{-1}$*s^{-1} or cm^6*$molecule^{-2}$*s^{-1})**	**Reference**
$N + O_3 \rightarrow NO + O_2$	$5.0*10^{-12}*\exp(-650/Tgas)$	6
$NO + NO_2 + M \rightarrow N_2O_3 + M$	$9.1*10^{-33}$	7
$N_2O_3 + M \rightarrow NO + NO_2 + M$	$1.9*10^{-7}*(Tgas/300)^{-8.7}*\exp(-4880/Tgas)$	8
$2NO_2 + M \rightarrow N_2O_4 + M$	$1.4*10^{-33}*(Tgas/300)^{-3.8}$	9
$N_2O_4 + M \rightarrow 2NO_2 + M$	$1.3*10^{-5}*(Tgas/300)^{-3.8}*\exp(-6460/Tgas)$	8
$N + O + M \rightarrow NO + M$	$1.0*10^{-32}*(300/Tgas)^{0.5}$	8
$NO_2 + NO_3 + M \rightarrow N_2O_5 + M$	$3.6*10^{-30}*(300/Tgas)^{4.1}$	9
$N_2O_5 + M \rightarrow NO_2 + NO_3 + M$	$1.3*10^{-3}*(Tgas/300)^{-3.5}*\exp(-11000/Tgas)$	8,9
$N_2(A^3\Sigma_u^+) + CO_2 \rightarrow CO + O$	$6.25*10^{-14}$	10

The following tables give the CO_2 and N_2 percentages in the mixture (1st and 2nd column), the calculated CO_2 and N_2 conversion (3th and 4th column), the calculated energy efficiency (column 5), the calculated NO concentration in parts per million (column 6), the calculated NO_2 concentration in parts per million (column 7), the calculated N_2O_3 concentration in parts per million (column 8), the calculated N_2O_5 concentration in parts per million (column 9) and the calculated N_2O concentration in parts per million (column 10).

a) 0-10 % N_2

CO_2 (%)	**N_2 (%)**	**χ CO_2 calc (%)**	**χ N_2 calc (%)**	**η calc (%)**	**NO (ppm)**	**NO_2 (ppm)**	**N_2O_3 (ppm)**	**N_2O_5 (ppm)**	**N_2O (ppm)**
100	0	4.12	-	3.8	-	-	-	-	-
99	1	4.20	0.46	3.8	43.46	9.72	0.006	14.26	2.99
98	2	4.23	0.37	3.8	63.91	14.41	0.013	26.04	5.96
97	3	4.26	0.32	3.8	76.83	17.45	0.018	37.02	8.59
96	4								
95	5	4.33	0.27	3.7	91.86	21.17	0.026	58.29	13.39
94	6								
93	7								
92	8	4.45	0.22	3.7	102.81	24.20	0.034	90.36	19.88
91	9								
90	10	4.53	0.21	3.7	106.81	25.51	0.037	112.37	23.79

b) 0-100 % N_2

CO_2 (%)	N_2 (%)	χ CO_2 calc (%)	χ N_2 calc (%)	η calc (%)	NO (ppm)	NO_2 (ppm)	N_2O_3 (ppm)	N_2O_5 (ppm)	N_2O (ppm)
100	0	4.12	-	3.8	-	-	-	-	-
90	10	4.53	0.21	3.7	106.81	25.51	0.037	112.37	23.79
80	20	5.03	0.18	3.7	114.50	29.35	0.046	233.39	38.68
70	30	5.65	0.17	3.6	115.47	31.76	0.050	373.38	47.36
60	40	6.42	0.17	3.5	113.21	33.43	0.051	528.66	51.92
50	50	7.34	0.17	3.3	107.68	34.18	0.050	690.55	53.83
40	60	8.46	0.16	3.1	98.29	33.66	0.045	841.94	53.91
30	70	9.83	0.16	2.7	84.05	31.20	0.036	952.65	52.26
20	80	11.61	0.14	2.1	63.61	25.83	0.022	964.41	48.28
10	90	14.19	0.09	1.3	34.88	15.57	0.007	741.02	39.92
0	100	-	0.00	-	-	-	-	-	-

c) 90-98 % N_2

CO_2 (%)	N_2 (%)	χ CO_2 calc (%)	χ N_2 calc (%)	η calc (%)	NO (ppm)	NO_2 (ppm)	N_2O_3 (ppm)	N_2O_5 (ppm)	N_2O (ppm)
10	90	14.19	0.09	1.3	34.88	15.57	0.007	741.02	39.92
9	91	14.53	0.09	1.2	31.46	14.15	0.006	694.31	38.63
8	92								
7	93	15.28	0.07	1.0	24.35	11.04	0.004	580.31	35.58
6	94								
5	95	16.19	0.05	0.7	16.98	7.59	0.002	433.21	31.72
4	96								
3	97	17.38	0.03	0.5	9.63	3.91	0.001	244.68	26.62
2	98	18.29	0.02	0.3	6.12	2.22	0.000	135.13	23.38

3. References

1 R. Snoeckx, R. Aerts, X. Tu and A. Bogaerts, *J. Phys. Chem. C*, 2013, **117**, 4957–4970.

2 U. Kogelschatz, *Plasma Chem. plasma Process.*, 2003, **23**, 1–46.

3 M. Ramakers, I. Michielsen, R. Aerts, V. Meynen and A. Bogaerts, *Plasma Process. Polym.*, 2015, **12**, 755–763.

4 S. Keller, P. Rajasekaran, N. Bibinov and P. Awakowicz, *J. Phys. D. Appl. Phys.*, 2012, **45**, 125202.

5 S. Heijkers, R. Snoeckx, T. Kozák, T. Silva, T. Godfroid, N. Britun, R. Snyders and A. Bogaerts, *J. Phys. Chem. C*, 2015, **119**, 12815–12828.

6 I. Stefanovic, N. ~K. Bibinov, A. ~a. Deryugin, I. ~P. Vinogradov, A. ~P. Napartovich and K. Wiesemann, *Plasma Sour. Sci. Technol.*, 2001, **10**, 406.

7 I. W. M. Smith and G. Yarwood, *Faraday Discuss. Chem. Soc.*, 1987, **84**, 205–220.

8 S. Teodoru, Y. Kusano and A. Bogaerts, *Plasma Process. Polym.*, 2012, **9**, 652–689.

9 R. Atkinson, D. L. Baulch, R. a. Cox, J. N. Crowley, R. F. Hampson, R. G. Hynes, M. E. Jenkin, M. J. Rossi and J. Troe, *Atmos. Chem. Phys. Discuss.*, 2003, **3**, 6179–6699.

10 G. Black, T. G. Slanger, G. a S. T. John and R. a Youngt, *Chem. Phys.*, 1969, **51**, 116–121.